



This article appeared in a journal published by Elsevier. The attached copy is furnished to the author for internal non-commercial research and education use, including for instruction at the authors institution and sharing with colleagues.

Other uses, including reproduction and distribution, or selling or licensing copies, or posting to personal, institutional or third party websites are prohibited.

In most cases authors are permitted to post their version of the article (e.g. in Word or Tex form) to their personal website or institutional repository. Authors requiring further information regarding Elsevier's archiving and manuscript policies are encouraged to visit:

<http://www.elsevier.com/authorsrights>



Good cycling performance of high-density arrays of Si microwires as anodes for Li ion batteries

Enrique Quiroga-González¹, Jürgen Carstensen, Helmut Föll*

Institute for Materials Science, Christian Albrechts University of Kiel, Kaiserstr. 2, 24143 Kiel, Germany

ARTICLE INFO

Article history:

Received 13 July 2012

Received in revised form 29 October 2012

Accepted 30 October 2012

Available online 8 November 2012

Keywords:

Si wire anode

Li ion battery

Wire array

High capacity

ABSTRACT

Optimized Si wire anodes have been prepared by macropore etching in p-Si and subsequent chemical/galvanic processing. The anodes have been optimized with respect to capacity, cycling performance and processing costs by fine-tuning the wire geometry. The optimized anodes have wires with $\approx 1 \mu\text{m}$ in diameter and length of $70 \mu\text{m}$; they are as densely spaced as possible regarding volume expansion and electrolyte penetration requirements. A stable capacity of 3150 mAh/g for 100 cycles has been reached during cycling to 75% of the maximum capacity. The operational range of the anodes is $0.11\text{--}0.7 \text{ V}$. Optimal charging conditions were established by cyclic voltammetry measurements and battery cycling tests.

© 2012 Elsevier Ltd. All rights reserved.

1. Introduction

The capacity of an anode for Li ion batteries is given by the amount of Li that can be incorporated into a unit mass or volume of the anode material. Silicon offers a nominal capacity of 4200 mAh/g , more than ten-fold [1] that of the 330 mAh/g of standard graphite anodes [2]. Furthermore, when this material is delithiated, it has a potential drop of only about 0.5 V . Despite these obvious advantages, bulk Si is useless as an anode, because the incorporation of Li leads to a volume expansion of up to a factor of 4, resulting in stress-produced fracture and subsequent rapid fading of the capacity.

In a groundbreaking paper Chan et al. showed in 2008 that this problem could be overcome by using nano-structured Si in the form of nanowires [1]. Si nanowires, while still increasing their volume fourfold during the incorporation of Li, do not fracture and show promising performance in battery tests. After this report substantial progress has been made concerning the production of nanostructured Si as anode material [3–9], often with morphologies different from freestanding Si wires. Generally, most Si anodes dealt with in the literature reach the maximum theoretical capacity of Si, at (slightly controversial) 4200 mAh/g [1,6,10] or 3574 mAh/g [11–13]. However, silicon wire anodes (SWAs) of several competing groups experience high capacity fading, going for example from the maximum capacity (first cycle) to 1700 mAh/g

within 50 charging/discharging cycles while still showing coulomb efficiencies above 90% [6]. Possibly the conductivity of the wires decreases dramatically upon cycling, or the contacting with the current collector is destroyed. The wires grown by vapor liquid solid (VLS) methods, for example, are just contacted at their bottom; the contact thus must be expected to support only small strains. New approaches therefore focus on some post processing of the wires [1,7], e.g. covering the wires with amorphous Si particles that act as “easy access” active material [14]. To overcome the fading problems, other Si anode approaches have been tested. For example, carbon nanofibers (electrical conductors) have been covered with amorphous Si [15,16]. Mixing Si particles with conducting materials [17], or mixing Si “wires” with carbon-based additives to improve the conductivity [18,19], has also been tried.

As will be shown here, our SWAs live through more than 100 cycles with less than 1% fading, without (costly) post-processing and with diameters ($\approx 1 \mu\text{m}$) far larger than the 300 nm deemed critical in [20].

It is clear that the Si wire anodes (SWAs) of the previous reports have not been optimized. An *optimized* SWA must meet the following conditions:

- Wires as long as possible and as thick as possible with the minimum of free space in between that is necessary to allow for volume expansion and some solid electrolyte interface (SEI) “coating”. Long wires are preferable because the anode capacity must take into account the weight of the current collector and the electrolyte. Thick wires are preferable because the ohmic resistance is smaller and they are easier to make. A minimum of free

* Corresponding author. Tel.: +49 431 8806175; fax: +49 431 8806178.

E-mail address: hfoell@tf.uni-kiel.de (H. Föll).

¹ ISE member.

space maximizes the capacity per volume and the capacity per weight, since it needs less electrolyte that contributes substantially to the total weight!

- It must be solidly connected to a current collector (preferably Cu) in such a way that substantial current densities ($1\text{--}10\text{ mA/cm}^2$) can be run into and out of the anode uniformly.
- Considering applications in commercial batteries, SWAs must have the potential of being mass-produced at reasonable costs.

From a performance point of view, freestanding Si microwires with optimized geometry are superior to anodes involving Si in other forms. From an application point of view, SWAs as reported here can be mass-produced at reasonable costs (roughly comparable to those of Si solar cells). The paper reports about the progress made in optimizing free-standing SWA anodes along the criteria given above.

2. Experimental details

Battery cycling tests were performed in half battery cells (using Li as the counter electrode). The electrolyte was LP30 (0.5 mL), which consists of 1 mol/L of LiPF_6 salt in a 1:1 solution of ethylenecarbonate and dimethylcarbonate. The separator was a glass fiber microfilter from Whatman, with pores of $1\text{ }\mu\text{m}$. If no other specified, the lithiation/delithiation tests were done under the following conditions: A current of $C/10$ (the current is calculated so that it takes 10 h to lithiate or delithiate) was used. For the lithiation a voltage limit of 0.11 V was given, while for the delithiation the voltage limit was 0.7 V. When the voltage limit was reached, the cycling was switched to potentiostatic mode, and this mode finished when the current decreased to 10%, or the capacity limit (4200 mAh/g) was accomplished. This is a standard way of charging commercial batteries to protect them from over-charging.

For the cyclic voltammetry tests, the same half battery cells as for the battery cycling tests were prepared.

3. Results and discussion

3.1. First generation optimized Si wire anodes

3.1.1. Production

The fabrication process of our SWA has been discussed in some detail in previous reports [8,9]. Cursorily, the steps of the fabrication process are:

- Anodically etching macropores into p-type (or n-type) Si wafers. For the macropore etching, the surface of the Si substrates should be pre-structured with “nuclei” (etch pits with inverted pyramid shapes), using (cheap) standard contact lithography and simple post processing. The main characteristics of the pores is an optimized pore diameter profile with two abrupt “diameter constrictions” and a diameter increase at the tip region of the pores. While pore profiling is an established technique by now, it should be mentioned that the relations between pore diameter and etching conditions (current, voltage, temperature and possibly illumination as function of time) are highly non-linear and not easily obtained.
- Chemical over-etching of porous Si until the pores touch and only the interstices = wires are left. The over-etching produces the Si wires by reducing the thickness of the pore walls until the pores merge. The etching of the pore walls is accomplished with a KOH based etchant, which acts anisotropically. The wires obtained are square-shaped in the cross section, with flat walls. Si between the pores at the positions of the “diameter constrictions” is not completely dissolved and provides

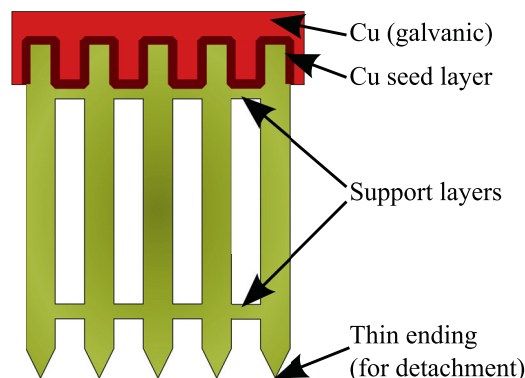


Fig. 1. Scheme of the Si wire anodes, indicating their main structural elements.

stabilizing planes that connect the Si wires in pre-selected depths (see Fig. 1). This prevents wire collapse due to “stiction” or the “wet hair effect” when the sample is taken out of the liquid. The enlarged diameter around the tip of the pores provides for very thin wires next to the remaining substrate. This allows detaching the array from the substrate in an easy way.

- Deposition of a Cu current collector. Since stiction is avoided, the surface of the wire array is still perfect and Cu can now be deposited on top of the array. Electrochemical processes were chosen because of general cost considerations, in addition to issues of process flexibility and adhesion of the films. A pre-condition for galvanic Cu deposition is electroless deposition of a Cu seed layer (see Fig. 1), since the Si wires behave as isolators in this process. As shown in Fig. 1, Cu is deposited between the wires down to the depth of the first support layer, allowing a good electrical and in particular mechanical contact.

Using the described concept for SWA production, optimized anodes were produced in a first iteration and described in [9]. Considering that the largest possible amount of active material is desired, the wires were produced as thick as possible, with the optimum lithographic structure for macropore etching for wires ($3\text{ }\mu\text{m}$ pitch). The wires had a diameter of $1.5\text{ }\mu\text{m}$, as shown in Fig. 2,

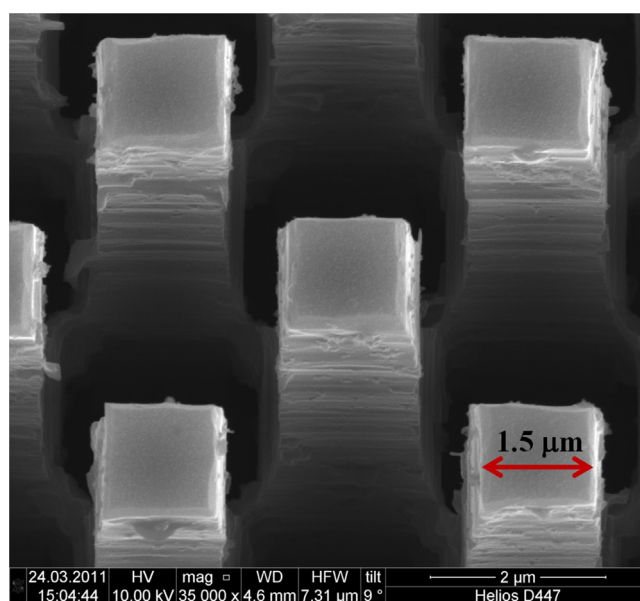


Fig. 2. Top view wires with thickness of $1.5\text{ }\mu\text{m}$. In this case the space left for expansion and SEI was marginally too small.

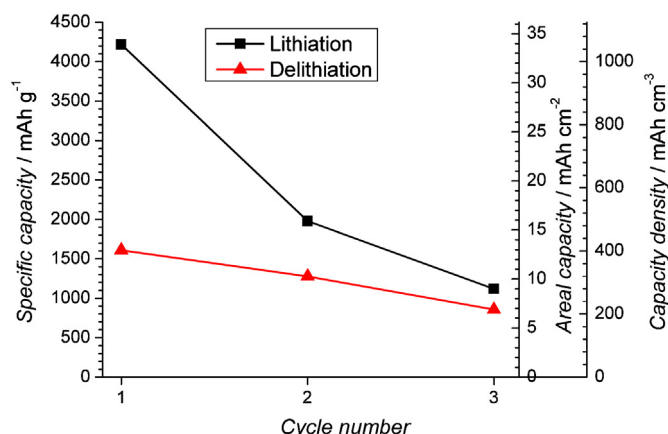


Fig. 3. Capacity of the first generation optimized SWA. Fast fading due to wire breakage is observed.

and were 150 μm long. By cyclic voltammetry it was evidenced that the produced anodes could withstand 60 cycles, exhibiting the lithiation/delithiation peaks characteristic for Si.

3.1.2. Battery cycling tests

In the battery tests the maximum theoretical capacity of Si of $\sim 4200 \text{ mAh/g}$ was easily reached in the first lithiation (see Fig. 3). The large diameters of the wires together with limited space for expansion had, as expected, a positive effect for the charge per area and per volume, but a negative effect for cycle stability, where relatively fast fading was observed. The problem could be traced to a small but persistent loss of pieces of the anodes (loss of active material), probably due to wire breakage because they touch when fully loaded with Li. This first generation SWAs had a length of 150 μm , a pitch of 3 μm , and a diameter of 1.5 μm , leading to a very high areal capacity of 33.7 mAh/cm^2 ; this capacity is in fact very high for good cycling performance due to the close-packing.

3.2. Second generation of SWAs with 1 μm diameter

There are several ways to address the problem of cracking outlined above. Among them we have: (1) covering the wires with an additional material which maintains them in one piece; (2) increasing the space between wires; (3) reducing the diameter of the wires. The first two possibilities require modifications of the structure of the already optimized process, and additionally they could not solve all the problems. The first solution requires finding an inactive material that works as membrane, and has the plasticity of polymers; afterwards its deposition should be optimized so that the wires are fully and homogeneously covered. This approach can avoid that the wires pulverize; nevertheless it is very possible that the cracks caused by stress will still exist, since the expansion is limited. The second solution could give enough space to the wires to “breathe”, but a completely new lithographic structure and etching concept should be found. On the other hand, it is not known if wires with so large diameters could stand the expansion stress. We opted for the third solution, since is the easiest to achieve, and is the most promising. The diameter of the wires was thus reduced to 1 μm .

3.2.1. Production

While the reduction of the wire diameter may appear to be a straightforward process, this is not the case. Simply over-etching the porous Si for longer times, for example, compromises the support layers and leads to wire collapse by stiction. This terminates the processing because chemical/electrochemical deposition of Cu

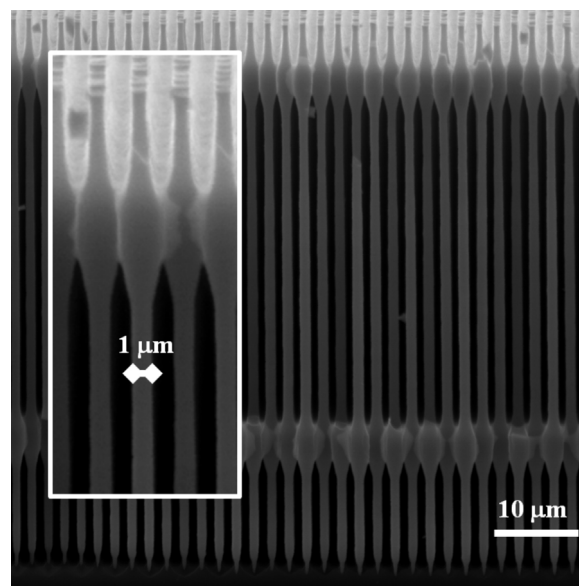


Fig. 4. Second generation of optimized wires with 1 μm diameter. A complex etching current–time profile is essential for their production, plus control of some other parameters.

on wire surface is no longer possible. Making the wires thinner requires some pore profile engineering that must be realized in many iterative optimizing steps. The support layer must stand longer etching times, or the amount of Si to be etched for obtaining thin wires should be small. For this purpose, the difference in diameter between the “pore constrictions” and the rest of the pores should be large. We have succeeded in making macropores with larger diameters while keeping the diameter of the pores at the constrictions constant. This was possible through the use of polyethyleneglycol as surfactant in the etchant for electrochemical etching. A SEM micrograph of the wires obtained after chemical etching is shown in Fig. 4. As can be observed, the wires have a diameter of 1 μm , and the support layers are well defined, securely avoiding collapse of the wires.

3.2.2. Determination of the SWA voltage operation range

Cyclic voltammetry tests were done with a scan rate of 0.1 mV/s in the range of 0–2 V for 3 cycles. Plots of the measurements are shown in Fig. 5a. From this figure it can be observed that just one peak, found at 1.17 V during the negative voltage sweep of the first cycle, is not repeated upon cycling. This represents a single irreversible event, which could be attributed to SEI formation, as will become clear later on. The rest of the peaks are found below 1 V.

To better observe the rest of the peaks, voltammograms with the same sweep rate, but in the range of 0–1 V were done. The experiment was performed for 10 cycles to test the stability of the anode. For visual purposes, just data from selected cycles are shown in Fig. 5b. Peaks labeled A and B are found during the negative voltage sweeps (sweep from high to low voltages) at around 0.23 V and 0.16 V, respectively. These peaks are related to the lithiation of Si and the formation of Li–Si alloys. Peaks C and D appear during the positive voltage sweeps at around 0.37 V and 0.53 V respectively. These two peaks are related to delithiation processes. The position of all the peaks is consistent with the reported values in the literature with slight deviations [6,19,21,22]. The largest deviation, most likely caused by size effects, occurs for peak B. For example, Si nanowires of 50 nm in diameter present a voltammetric peak below 35 mV, presumably due to the formation of $\text{Li}_{22}\text{Si}_5$ [6,21]. But other reports indicate that the maximum lithiation produces

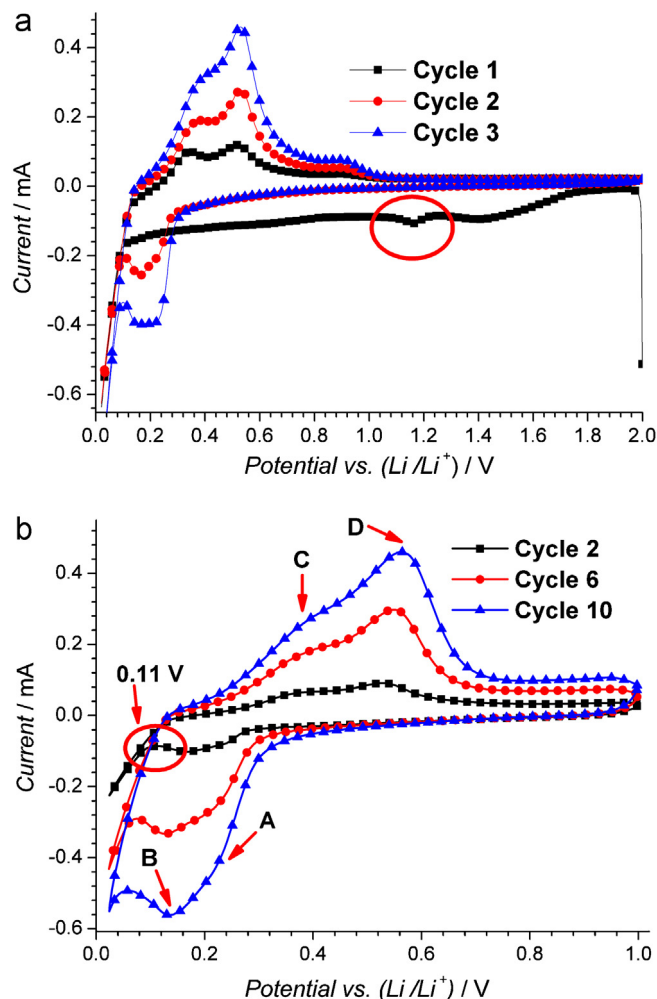


Fig. 5. Cyclic voltammograms of half battery cells with a second generation SWA. (a) Experiment performed in the range of 0–2 V. An irreversible event (encircled region) is observed during the negative sweep of the first cycle, at a voltage of 1.17 V; it corresponds to SEI formation. The rest of the peaks are observed below 1 V. (b) Experiment performed in the range of 0–1 V, to better observe the lithiation/delithiation events. The minimum operational voltage is around 0.11 V and the maximum occurs around 0.7 V. The lithiation peaks A and B at 0.23 V and 0.16 V, and the delithiation peaks C and D at 0.37 V and 0.53 V are observed.

a potential slightly below 50 mV, given by the formation of Li₁₅Si₄ [23]. For bigger particles it has been found that this potential limit is 70 mV [24]. From this survey it is suggestive to assume that the potential of the Si anodes in batteries depends critically on their size, strain and the crystallization of Li–Si phases. The finding of the same amount of peaks in the positive and negative sweeps may indicate that the processes are reversible. These peaks appear all the time, with small shifts upon cycling.

From cycle 2 it can be observed that the minimum voltage after peak B, is around 0.11 V. Below this voltage the negative current increases rapidly, probably due to direct deposition of Li on the current collector. The minimum voltage shifts upon cycling due to a constant change of the electrical conductivity of the wires. The maximum voltage after peak D is around 0.7 V. After this point no processes related to the alloying/de-alloying of Si with Li occur.

In addition a galvanostatic lithiation/delithiation test at C/10 (the lithiation or delithiation takes 10 h) with no voltage or charging level constraints was performed. The resulting voltage behavior with time is shown in Fig. 6a for the lithiation and in Fig. 6b for the delithiation process. With a lithiation rate of C/10 it was expected that the total charging of the anode (4200 mAh/g) could

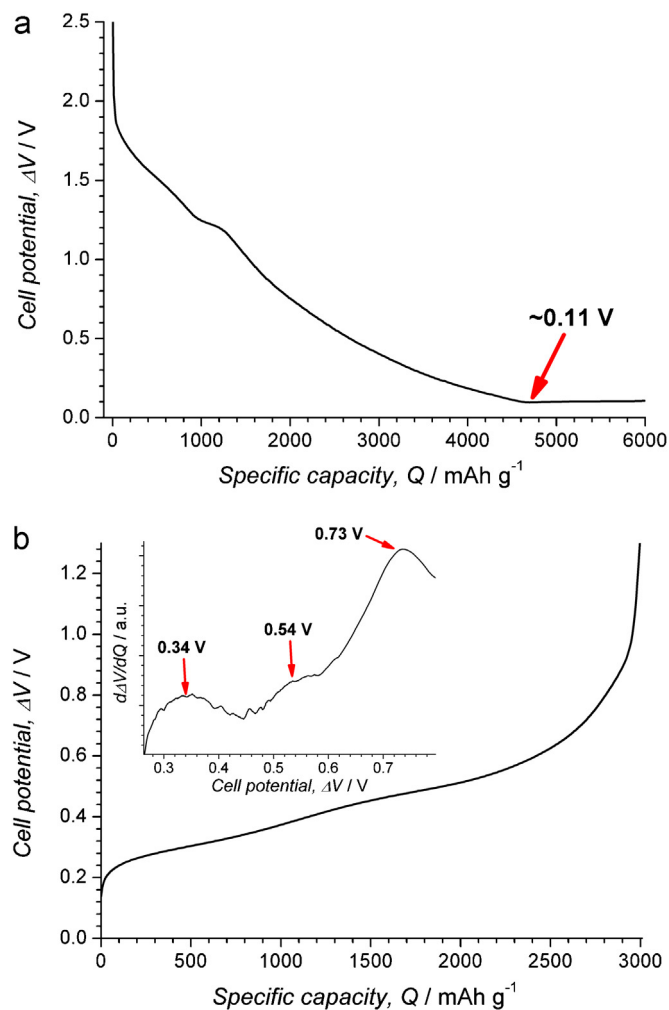


Fig. 6. Voltage vs time curves when lithiating/delithiating the second generation SWAs with constant current of C/10, and without voltage limits. (a) First lithiation. The minimum possible voltage is described with the plateau found at around 0.11 V. An additional plateau is observed at 1.2 V, in agreement with the cyclic voltammetry experiments, corresponding to SEI formation. (b) First delithiation. The inset presents the double derivative of voltage in respect to capacity, for an easier identification of the changes in slope. Three peaks can be observed. The first two peaks can be assigned to lithiation processes, and the third peak to the end point of these processes.

be accomplished in 10 h, indicated by the voltage staying constant. In our test a constant voltage of 0.11 V is obtained after ~11 h. The additional charging time could be due to the charge used for the SEI formation and/or small errors at weighting the anode to calculate the capacity. After 0.11 V has been reached, some current continues to flow but appears to be mainly shunt current. In some experiments we left this current flowing for additional 14 h but did not observe a reduction of the potential. This confirms that the minimum voltage of the present SWA vs Li is 0.11 V, in agreement with the cyclic voltammetry experiments; it may change, however, from cycle to cycle, as these last results also suggest. An additional voltage plateau is found around 1.2 V. This event is confirmed by a peak found at 1.17 V during the first cycle in the cyclic voltammetry tests (see Fig. 5a). As this process occurs only during the first negative voltage sweep, one may say that the involved process is irreversible. This process can be associated to SEI formation, which may be responsible for the irreversible losses during the first cycle of battery cycling tests, presented in Section 3.2.3.

The voltage curve of the delithiation process exhibits two changes in slope (see Fig. 6b). The voltage of the events is elucidated

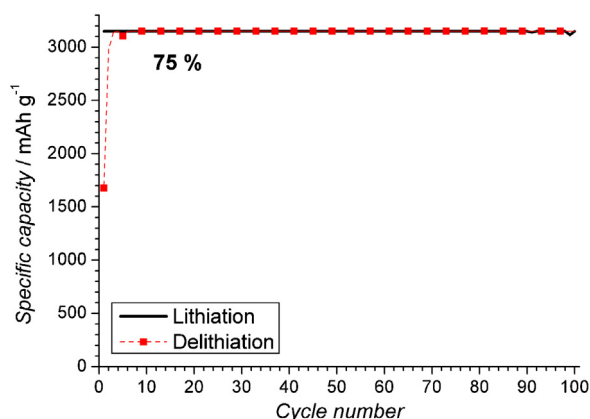


Fig. 7. Cycling performance of the optimized second generation SWAs with C/10 current for the first 4 cycles and C/2 current for the following ones. The capacity was limited to 75%. Under these conditions the fading is close to zero even after 100 cycles.

with the second derivative of the voltage in respect to the charge, plotted as inset in Fig. 6b. The first two peaks of this last curve indicate the starting points of the peaks found during the positive voltage sweeps of the cycling voltammograms (Fig. 5b), corresponding to delithiation events. The third peak, found at around 0.73 V, represents the end of the delithiation process, and coincides with the end of the delithiation peaks found by cyclic voltammetry.

Taking the results of cyclic voltammetry and galvanostatic lithiation/delithiation together, it appears that claim our optimized SWA anode operate in the range of 0.11–0.7 V. It is then preferable to cycle the anode in this range to be sure that the current flowing is charging the anode, and to not damage it.

3.2.3. Battery performance

Standard battery cycling experiments with the second generation optimized SAWs were performed in the operational voltage regime of 0.11–0.7 V using a charging current of C/10 (0.63 mA/cm²) during the first 4 cycles and a current of C/2 (3.15 mA/cm²) during the following ones, always at ambient temperature. The lithiation/delithiation was switched to a potentiostatic mode when the voltage limits were reached, and this mode finished when the current decreased to 10%, or the capacity limit was accomplished. Fig. 7 shows a curve of the capacity of the anodes lithiated to 75% of their maximum capacity. As can be observed in the figure, the capacity remains constant for 100 cycles, with coulomb efficiency of over 99% after cycle 2. An irreversible loss of 46% is observed in the first cycle, probably due to the formation of a SEI layer on the Si wires, and some base Si–Li phases, which are an important structural part of the wires for the next cycles (the wires are not totally delithiated). This SAWs exhibit the same large gravimetric capacity as thinner SAWs. Surprisingly, they have a good long term stability at relatively fast cycling rates, although the wires are much thicker than the 300 nm assumed to be the maximum possible dimension for good performance [20].

The SAWs of second generation presented in this paper have a length of 70 μm , which can easily be increased to at least 150 μm (as for the first generation SAWs). They have a pitch of 3 μm and a diameter of 1 μm , leading to an areal capacity of 6.3 mAh/cm². Increasing the length to 150 μm would result in a capacity of 13.5 mAh/cm², presumably larger than any SAWs.

The slow charging rate for the first cycles is indicated to allow a proper lithiation of the wires, and to minimize cracks produced by rapid stresses. After the first cycles the wires probably become amorphous, and attain a size that remains almost constant in the

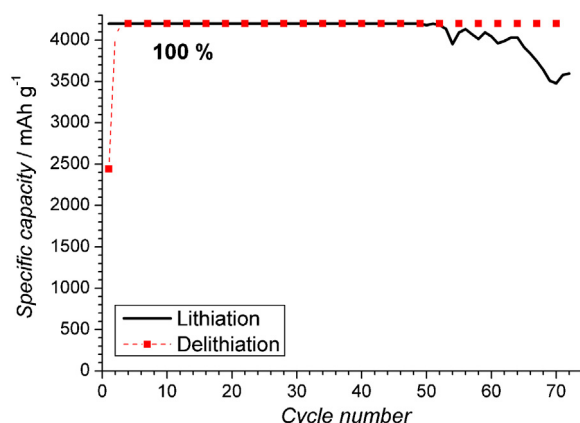


Fig. 8. Cycling performance of the Si wire anodes, with C/10 current for the first 4 cycles and with C/2 current for the following ones. The capacity was limited to 100%.

following cycles. Cycling to 75% of the maximum possible capacity may be good for always keeping some Li in the wires, and thus a base Li–Si alloy structure; this could minimize stresses caused to phase transitions.

3.2.4. Operation under extreme conditions

To confirm the selection of the charging conditions of the measurement of Fig. 7, other measurements at extreme conditions were performed. Fig. 8 shows the charging performance of the anodes under similar conditions to those of the test of Fig. 7, with the only difference that the limit of capacity was set to 100%. Under these conditions the anode performs very well up to 50 cycles, but some fading starts to occur after then. As can be observed from the figure, after cycle 51 there is more charge going out from the anode than what goes in during lithiation. One can infer that this behavior is due to increasing massive shunts, maybe caused by the growth of dendrites. Mass loss produced by wire fracturing could have some effect too.

Fig. 9 shows a plot of the capacity with the cycle number, limiting the capacity to 75%, but cycling with a rate of C/2 from the first cycle. As can be observed, under these conditions some fading occurs already after the first cycles, and losses remain at constant rate upon further cycling. Some stress-induced cracks may have been produced during the first cycle, due to the rapid lithiation, and consequently rapid expansion of the wires. In summary, for the present stage, measurement conditions exemplified in Fig. 7 are around the optimum.

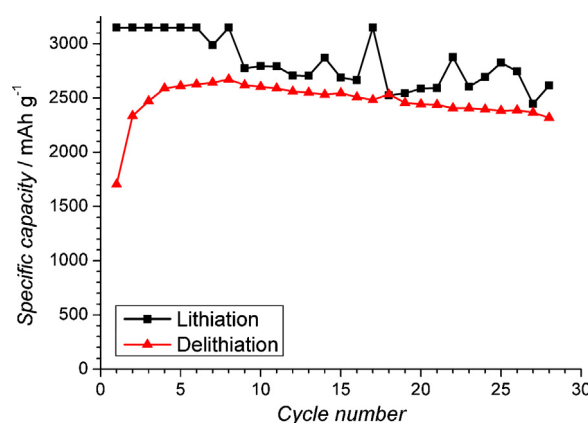


Fig. 9. Cycling performance of the optimized second generation SWAs with C/2 current for all the cycles. The capacity was limited to 75%.

4. Conclusions

Battery tests on first generation SWAs revealed several limitations for good stability, which could all be overcome by changing the pore geometry and implicitly the wire geometry after the chemical overetching. For the second generation SWAs most importantly the diameter of the wires had to be reduced while preserving the mechanical stability given by support layers. The wire tips had to remain large in order to allow for good embedding in a galvanically deposited Cu layer serving as current collector. The length of the wires can be easily controlled between 70 μm and at least 150 μm , allowing for capacities per area up to 13.5 mAh/cm².

Although literature results expect an upper limit of wire diameter for stable SWAs of around 300 nm, our 1 μm thick wires show a remarkable cycling performance. The capacity fade is almost zero after 100 cycles, using a C/2 charging current. For this superior performance to be obtained, of course optimized cycling conditions had to be found. These results are real challenges for all other SWA concepts.

Acknowledgements

The authors want to acknowledge the German Federal Ministry of Education and Research (BMBF) for the economical support provided through the “AlkaSuSi” project. The economical support of the German Science Foundation (DFG) as part of the special research field 855 “magnetoelectric composite materials – biomagnetic interfaces of the future” is also appreciated. They also want to thank Sandra Nöhren and Iris Hölken for their technical support in the preparation of the anodes.

Appendix A. Supplementary data

Supplementary data associated with this article can be found, in the online version, at <http://dx.doi.org/10.1016/j.electacta.2012.10.154>.

References

- [1] C.K. Chan, H. Peng, G. Liu, K. McIlwrath, X.F. Zhang, R.A. Huggins, Y. Cui, High-performance lithium battery anodes using silicon nanowires, *Nature Nanotechnology* 3 (2008) 31.
- [2] B.A. Boukamp, G.C. Lesh, R.A. Huggins, All-solid lithium electrodes with mixed-conductor matrix, *Journal of the Electrochemical Society* 128 (1981) 725.
- [3] H. Föll, H. Hartz, E.K. Ossei-Wusu, J. Carstensen, O. Riemenschneider, Si nanowires arrays as anodes in Li ion batteries, *Physica Status Solidi – Rapid Research Letters* 4 (2010) 4.
- [4] R. Ruffo, S.S. Hong, C.K. Chan, R.A. Huggins, Y. Cui, Impedance analysis of silicon nanowire lithium-ion battery anodes, *The Journal of Physical Chemistry C* 113 (2009) 11390.
- [5] R. Huang, X. Fan, W. Shen, J. Zhu, Carbon-coated silicon nanowire array films for high-performance lithium-ion battery anodes, *Applied Physics Letters* 95 (2009) 133119.
- [6] K. Kang, H.S. Lee, D.W. Han, G.S. Kim, D. Lee, G. Lee, Y.M. Kang, M.H. Jo, Maximum Li storage in Si nanowires for the high capacity three-dimensional Li-ion battery, *Applied Physics Letters* 96 (2010) 053110.
- [7] Y. Yang, M.T. McDowell, A. Jackson, J.J. Cha, S.S. Hong, Y. Cui, New nanostructured Li₂S/silicon rechargeable battery with high specific energy, *Nano Letters* 10 (2010) 1486.
- [8] H. Föll, J. Carstensen, E. Ossei-Wusu, A. Cojocaru, E. Quiroga-Gonzalez, G. Neumann, Optimized Cu-contacted Si nanowire anodes for Li ion batteries made in a production near process, *Journal of the Electrochemical Society* 158 (2011) A580.
- [9] E. Quiroga-Gonzalez, E. Ossei-Wusu, J. Carstensen, H. Föll, How to make optimized arrays of Si wires suitable as superior anode for Li-ion batteries, *Journal of the Electrochemical Society* 158 (2011) E119.
- [10] H. Ghassemi, M. Au, N. Chen, P.A. Heiden, R.S. Yassar, In situ electrochemical lithiation/delithiation observation of individual amorphous Si nanorods, *ACS Nano* 5 (2011) 7805.
- [11] M.T. McDowell, S.W. Lee, C. Wang, Y. Cui, The effect of metallic coatings and crystallinity on the volume expansion of silicon during electrochemical lithiation/delithiation, *Nano Energy* 1 (2012) 401.
- [12] K. Evanoff, A. Magasinski, J. Yang, G. Yushin, Nanosilicon-coated graphene granules as anodes for Li-ion batteries, *Advanced Energy Materials* 1 (2011) 495.
- [13] R. Chandrasekaran, A. Magasinski, G. Yushin, T.F. Fuller, Analysis of lithium insertion/deinsertion in a silicon electrode particle at room temperature, *Journal of the Electrochemical Society* 157 (2010) A1139.
- [14] L. Hu, H. Wu, S.S. Hong, L. Cui, J.R. McDonough, S. Bohy, Y. Cui, Si nanoparticle-decorated Si nanowire networks for Li-ion battery anodes, *Chemical Communications* 47 (2011) 367.
- [15] L.-F. Cui, Y. Yang, C.-M. Hsu, Y. Cui, Carbon-silicon core-shell nanowires as high capacity electrode for lithium ion batteries, *Nano Letters* 9 (2009) 3370.
- [16] P.-C. Chen, J. Xu, H. Chen, C. Zhou, Hybrid silicon-carbon nanostructured composites as superior anodes for lithium ion batteries, *Nano Research* 4 (2011) 290.
- [17] S. Zhou, X. Liu, D. Wang, Si/TiSi₂ Heteronanostructures as high-capacity anode material for Li ion batteries, *Nano Letters* 10 (2010) 860.
- [18] N. Ding, J. Xu, Y. Yao, G. Wegner, I. Lieberwirth, C. Chen, Improvement of cyclability of Si as anode for Li-ion batteries, *Journal of Power Sources* 192 (2009) 644.
- [19] C.K. Chan, R.N. Patel, M.J. O'Connell, B.A. Korgel, Y. Cui, Solution-grown silicon nanowires for lithium-ion battery anodes, *ACS Nano* 4 (2010) 1443.
- [20] J. Graetz, C.C. Ahn, R. Yazami, B. Fultz, Highly reversible lithium storage in nanostructured silicon, *Electrochemical and Solid-State Letters* 6 (2003) A194.
- [21] M. Green, E. Felder, B. Scrosati, M. Wachtler, J.S. Moreno, Structured silicon anodes for lithium battery applications, *Electrochemical and Solid-State Letters* 6 (2003) A75.
- [22] H. Chen, Y. Xiao, L. Wang, Y. Yang, Silicon nanowires coated with copper layer as anode materials for lithium-ion batteries, *Journal of Power Sources* 196 (2011) 6657.
- [23] M.N. Obrovac, L. Christensen, Structural changes in silicon anodes during lithium insertion/extraction, *Electrochemical and Solid-State Letters* 7 (2004) A93.
- [24] V.L. Chevrier, J.R. Dahn, First principles model of amorphous silicon lithiation, *Journal of the Electrochemical Society* 156 (2009) A454.